Original Research *Feature article*

c-Src inhibitor PP2 inhibits head and neck cancer progression through regulation of the epithelial–mesenchymal transition

SunYoung Lee[1], Sunjung Park[1], Jae-Sung Ryu[1], Jaegu Kang[1], Ikhee Kim[1], Sumin Son[1], Bok-Soon Lee[2], Chul-Ho Kim[3] and Yeon Soo Kim[1]

[1]Department of Otorhinolaryngology, College of Medicine, Konyang University Hospital, Konyang University Myunggok Medical Research Institute, Daejeon 35365, Republic of Korea; [2]School of Medicine and Health Sciences, The George Washington University, Washington, DC 20037, USA; [3]Department of Otolaryngology, School of Medicine, Ajou University, Suwon 16499, Republic of Korea
Corresponding author: Yeon Soo Kim. Email: ionskim@gmail.com

Impact statement

Despite numerous studies of head and neck squamous cell carcinoma (HNSCC)treatment, the treatment outcome has remained virtually unchanged, and the 5-year survival rate with current treatment strategies is only 40%. 4-amino-5-(4-chlorophenyl)-7-(dimethylethyl)pyrazolo[3,4-d] pyrimidine (PP2) is a selective inhibitor of proto-oncogene tyrosine-protein kinase Src (c-Src) which was initially used to treat myelogenous leukemia. PP2 has recently been studied as a cancer treatment. In our experiment, cancer cell growth and progression, including migration and invasion, were inhibited by PP2. In addition, cell apoptotic activity was increased, and cleaved caspase-3 expression was upregulated by PP2. Our findings demonstrated that PP2 inhibited the cell growth and progression in HNSCC via regulation of epithelial–mesenchymal transition.

Abstract

Head and neck squamous cell carcinoma (HNSCC) is one of the most common cancer, causing considerable mortality and morbidity worldwide. Although HNSCC management has been extensively studied, the treatment outcomes have not improved – the 5-year survival rate of patients with HNSCC is 40%. Recent studies on the development of a novel HNSCC treatment have highlighted proto-oncogene tyrosine-protein kinase Src (c-Src) as one of the major therapeutic targets. However, the clinical efficacy of c-Src inhibitors against HNSCC was not comparable to that obtained *in vitro*. Furthermore, the molecular mechanisms underlying the efficacy of c-Src inhibitors remain elusive. In this study, we assessed the efficacy of 4-amino-5-(4-chlorophenyl)-7-(dimethylethyl)pyrazolo[3,4-d] pyrimidine (PP2), a selective c-Src inhibitor on HSNCC. Nine HNSCC cell lines (SNU1041, Fraud, SNU46, SNU1076, SNU899, SCC1483, YD15, YD9, and YD10-) were screened, and the effects of PP2 were evaluated using wound healing, apoptosis, and invasion assays. Western blot analysis of downstream markers was conducted to assess the specific mechanism of action of PP2 in HNSCC. The therapeutic efficacy of PP2 was further evaluated in xenograft mice. PP2 reduced tumor cell growth both *in vitro* and *in vivo*. Furthermore, it enhanced tumor cell apoptosis in cell lines and prevented metastasis in mice. PP2 also regulated the epithelial–mesenchymal transition pathway downstream of c-Src. More specifically, in SCC1483 and YD15PP2 HNSCC cell lines, PP2 exposure downregulated Erk, Akt/Slug, and Snail but upregulated E-cadherin. These results suggest that PP2 inhibits cell growth and progression in HNSCC by regulating the epithelial–mesenchymal transition pathway.

Keywords: PP2, head and neck cancer, HNSCC, c-Src inhibitor, epithelial–mesenchymal transition, xenograft

***Experimental Biology and Medicine* 2023; 248: 492–500. DOI: 10.1177/15353702221139183**

Introduction

The head and neck cancers (HNCs) occurring in the nasal area, paranasal sinuses, oral cavity, salivary glands, pharynx, and larynx are collectively referred to as head and neck squamous cell carcinoma (HNSCC). This malignant neoplasm is the sixth most common type of cancer with increasing incidence worldwide, affecting ~600,000 new cases each year.[1] Unfortunately, the 5-year survival rate of HNSCC is only 40% despite currently available therapeutic strategies, including surgery, chemotherapy, radiation, and combination regimens, such as chemoradiation.[2] It is, therefore, imperative that new drug targets and therapeutics are identified to treat HNSCC.

The proto-oncogene tyrosine-protein kinase Src (c-Src), a 60-kDa non-receptor tyrosine kinase regulating various carcinogenic processes, such as proliferation, survival, motility, and the function of fully differentiated cells, is one of the promising molecular targets for HNSCC treatment.[3] c-Src was first identified as the cellular form of v-Src, a transgene product of the avian Rous sarcoma virus.[4] Src comprises one NH2-terminal region, two conserved Src homology domains, and one tyrosine kinase (TK) protein domain. Src is regulated via a C-terminal TK (Y527, corresponding to human Y530),

which upon phosphorylation by the C-terminal Src kinase (Csk), leads to a less active conformation. The mutated and constitutively active forms of c-Src are associated with various human cancers, including HNSCC; however, it is inactive under basal conditions.[5]

In HNSCC, c-Src activation promotes proliferation, invasion, angiogenesis, and cancer metastasis.[6–8] Furthermore, in patients with HNSCC, c-Src activation leads to poor differentiation and lymph node metastases.[9] c-Src inhibition suppresses HNSCC proliferation, invasion, and migration. More specifically, c-Src inhibition abrogated the proliferation and invasion of HNSCC cells *in vitro*.[10] However, clinical studies of c-Src inhibition in cancer have not been promising.

For instance, the Phase I, but not Phase II, testing of saracatinib (AZD0530), a potent drug that downregulates activated Src,[11] is complete. However, available Phase II data suggest AZD0530 is ineffective against HNSCC.[12] AZD0530 blocks the Src/Abelson murine leukemia viral oncogene homolog 1 (Abl)-breakpoint cluster region (Bcr) kinase pathway.[11] Similarly, dasatinib (BMS-354825), an inhibitor of Src and CD117, suppressed the activity of phosphorylated c-Src and inhibited both tumor cell proliferation and invasion in preclinical trials.[13] Reportedly, as the activation of Src is implicated in various solid tumors, it has emerged as a promising therapeutic target. The elucidation of the mechanisms underlying its activation has fostered the development of Src targeting drugs. Drugs, including BMS-354825, AZD0530, bosutinib (SKI-606), KX2-391, and XL228, that can inhibit the Src family kinases, are currently being investigated for their efficacy against various solid tumors. In human trials, dasatinib monotherapy has been shown to inhibit c-Src; however, it did not affect tumor growth.[14] Recent studies reported a relation between c-Src expression and epidermal growth factor receptor (EGFR) inhibitor resistance in cancers, including lung, gastric, colon cancer, and HNSCC.[15–18] c-Src overexpression conferred erlotinib (Tarceva) resistance, an EGFR TK inhibitor, while c-Src knockdown enhanced the sensitivity to erlotinib both *in vitro* and *in vivo*.[18] Likewise, inhibition of c-Src has anticancer effects against colon and gastric cancers that are resistant to EGFR-targeting therapeutics.[16,17]

The proto-oncogene Src and its kinase family play a major role in cancer cell proliferation, invasion, and chemoresistance. The selective c-Src inhibitor 4-amino-5-(4-chlorophenyl)-7-(dimethylethyl) pyrazolo[3,4-d] pyrimidine (PP2) was initially used to treat myeloid leukemia.[19] Recent studies have demonstrated that PP2 inhibits the growth and invasion of cancer cell lines, including those of HNSCC origin.[7,20–22] In this study, we investigated the anticancer effects and underlying mechanisms of the c-Src inhibitor PP2 against HNSCC.

Materials and methods

The rabbit anti-protein kinase B (AKT) (#9272), rabbit anti-phosphorylated AKT (pAKT) (#9271), rabbit anti-Actin (#4970), rabbit anti-E-cadherin (#3195), rabbit anti-N-cadherin (#4061), rabbit anti-Vimentin (#3932), mouse anti-extracellular signal-regulated kinase (ERK) (#9107), mouse anti-phosphorylated ERK (pERK) (#9106), rabbit anti-Slug (#9585), rabbit anti-Snail (#3879), rabbit anti-PARP (#5625), and rabbit anti-cleaved caspase-3 (#9661) primary antibodies were purchased from Cell Signaling (Cell Signaling Technology, MA, USA). Other antibodies, including mouse anti-c-Src (#sc8056), mouse anti-phosphorylated c-Src(p-csrc) (#sc81521). The secondary antibodies used in this study were acquired from Santa Cruz Biotechnology (Dallas, TX, USA). PP2 was purchased from Sigma (#P0042; Sigma, MO, USA) and suspended in phosphate-buffered saline (PBS)/DMSO at stock concentrations of 5, 10, and 20 μM.

Cell lines and cell culture

The following human HNSCC cell lines were obtained from the Korea Cell Line Bank (Seoul, Korea): YD9, YD15, YD10-B, SNU1076, SNU46, SNU899, and SNU1041. FaDu cells were purchased from the American Type Culture Collection (ATCC, Manassas, VA, USA), and SCC1483 cells were provided by Prof. Se-Heon Kim (Yonsei University, Korea). Cell lines were routinely cultured in RPMI 1640 (#11875-093; Gibco/Invitrogen, Carlsbad, CA, USA), except for SCC1483s cells, which were maintained in Dulbecco's Modified Eagle's Medium/Nutrient Mixture F-12 (DMEM/F12; #12634-010; GIBCO/Invitrogen), and FaDu cells, which were maintained in Minimum Essential Medium (MEM; #11095-080; GIBCO/Invitrogen). All growth media were supplemented with 10% fetal bovine serum (FBS; #16000-044; GIBCO/Invitrogen) and antibiotic-antimycotic solutions (#15240-062; GIBCO). Cells were incubated at 37 °C and 5% CO_2 under humidified conditions.

Cell viability assay

Cells were seeded into 96-well plates at a density of 5×10^3 cells/well and allowed to reach confluence. Cells were then exposed to PP2 at the indicated concentrations for 24, 48, or 72 h. After exposure, cell viability was assessed using a cell counting kit-8 (CCK8; #96992; Sigma) following the protocol provided with the kit. Briefly, CCK8 solution was added to the wells containing the cell suspension, and the plates were incubated for 1 h. Subsequently, the optical density was measured using the Bio-Tek microplate reader (Winooski, VT, USA). Data are presented as a percentage relative to the control cells.

Wound-healing assay

Cells were seeded into 12-well plates at a density of ~5×10^4 cells/well, grown to confluence, and then deprived of serum for 24 h. The wounds were generated using sterile 200-μL pipette tips and washed with PBS, followed by exposure to PP2 or vehicle control (PBS/DMSO) for 24 h. Cells were stained with crystal violet (#V5265; Sigma), and the wound-healing area was examined via light microscopy. Each experiment was completed in triplicate.

Invasion assay

Cell invasion capacity was evaluated using Matrigel-coated Transwell invasion chambers (8 μm pore; #354480; Corning, MA, USA) as previously described.[23] SCC1483 or YD-15 cells were treated with PP2 or vehicle control (DMSO/PBS) for 24 h. After incubation, cells were fixed with formalin and stained with crystal violet. The number of invading cells was counted in three randomly selected representative fields per insert. Each assay was performed in triplicate.

Apoptosis analysis

Apoptotic cell death was detected using the Annexin V-FITC Apoptosis Staining/Detection Kit (#ab14085; Abcam, MA, USA) with propidium iodide (PI) staining, as previously described.[24] Cells were seeded in 10 cm-dish plates, allowed to reach confluence, and then exposed to PP2 for 24 h. Cells were harvested, washed with cold PBS, and stained with annexin V-FITC and PI at room temperature for 15 min in the dark. Early and late apoptosis was then quantified according to manufacturer instructions using a FACS system (Beckman Coulter, CA, USA)

Western blot analysis

Western blot analysis was performed following a previously described method[25] using the anti-actin, anti-p-c-Src, anti-c-Src, anti-cleaved caspase 3, anti-cleaved anti-PARP, anti-Slug, anti-Snail1, anti-E-cadherin, anti-N-cadherin, anti-Vimentin, anti-p-Erk, Erk, anti-p-Akt, and anti-Akt primary antibodies and peroxidase-conjugated secondary antibodies. β-Actin was employed as a housekeeping control, and the bands were quantified using Image J software normalized to β-actin.

Tumor xenograft mouse model

The protocol for animal studies was approved by the Ethics Committee for Animal Care and Use (P-20-34-A-01), Konyang University, Daejeon, Republic of Korea. The tumor xenograft mouse model was established as previously described.[26] Six-week-old male BALB/c nude mice were acquired from Orient Bio (Seongnam, Republic of Korea). After acclimatization for 7 days, the mice were subcutaneously injected with SCC1483 cells (1×10^4 cells/well). Seven days post-injection when the SCC1483 grafts developed into palpable tumors, mice in each group were randomly divided into treatment and control groups ($n = 5$ in each group). The control group received 1% DMSO. The mice in the treatment group were intraperitoneally injected with a single dose of 10 mg/kg PP2 daily. Mice in both groups were treated for 2 weeks, and body weight and tumor size were monitored daily. Finally, mice were sacrificed after 2 weeks, and the tumor tissues were excised.

Terminal deoxynucleotidyl transferase (TdT) dUTP Nick-End Labeling (TUNEL) assay

The TUNEL assay was performed following the protocols described in a previous study.[27] In situ Cell Death Detection Kit (Roche, Mannheim, Germany) was used for TUNEL assay on the cryo-preserved tissues following the manufacturer's instructions. The green-stained apoptotic cells were detected using a fluorescence microscope (Zen imaging software, Carl Zeiss, Microscopy GmbH, Jena, Germany).

Immunofluorescence

For immunofluorescence staining, tumor sections were washed three times in PBS (5 min per wash) and incubated for 1 h in blocking buffer (3% BSA #A7030, Sigma; 0.2% Triton X100 in PBS), followed by overnight (at 4 °C) incubation with primary antibodies. Afterward, the sections were washed three times with PBS and incubated for 1 h with Alexa 488 (#150113, Abcam) or Alexa 647 (#150079, Abcam) conjugated secondary antibodies. The sections were washed twice with PBS and stained with DAPI (2 μg/mL) for 5 min. Prior to use, the primary antibodies were diluted to 1:50 in the blocking buffer, and the secondary antibodies were diluted to 1:400 in PBS. Afterward, they were rinsed in water, the coverslips were mounted onto glass slides using mounting media (#TA-030-FM, Thermo), the slides were observed using a Zeiss Confocal microscope, and the images were captured. Zen imaging software (Carl Zeiss, microscopy GmbH, Jena, Germany) was used to analyze the images.

Statistical analysis

The data are presented as the mean ± standard error of the mean, as indicated. The data were analyzed using analysis of variance with Tukey's multiple comparisons test and Student's *t*-tests. The threshold for statistical significance was set at $p < 0.05$. The statistical analyses were performed using GraphPad Prism 5.0 software (GraphPad Software, CA, USA).

Results

c-Src phosphorylation in HNSCC

The phosphorylated and total c-Src levels were assessed in nine HNSCC cell lines (SNU1041, Fraud, SNU46, SNU1076, SNU899, SCC1483, YD15, YD9, and YD10-B). The results demonstrated that the c-Src level was increased in all HNSCC cell lines, and the highest c-Src phosphorylation was observed in SCC1483 and YD15 cell lines (Figure 1(a) and (b)). PP2 caused cell death in most cell lines.

PP2 suppresses growth and induces apoptosis in HNSCC cell lines

To determine whether c-Src inhibition via PP2 had anticancer effects, we assessed its effects on tumor cell growth. PP2 suppressed c-Src phosphorylation in SCC1483 and YD15 cell lines that exhibited the highest c-Src phosphorylation. The inhibitory effect of PP2 on c-Src phosphorylation in cell lines was confirmed using western blot analysis (Figure 2(a)). Furthermore, PP2-induced c-Src inhibition effectively suppressed tumor cell growth. The evaluation of apoptosis using annexin V-FITC and PI staining and flow cytometry revealed that PP2 exposure significantly increased the number of early and late apoptotic cells, with a 4.36- and 10.34-fold increase in apoptotic SCC1483 and YD15 cells relative to controls (Figure 2(b)). Caspase-3 and PARP show a pivotal role in the intrinsic apoptosis pathway. Western blot analysis demonstrated a significant increase in caspase-3 (17.19 kDa) and cleaved PARP (89 kDa) levels in PP2-treated SCC1483 and YD15 cell lines compared with controls (Figure 2(c)). Taken together, these findings indicated that PP2 suppressed HNSCC cell growth and induced cancer cell apoptosis via the upregulation of caspase-3 and PARP.

PP2 suppresses HNSCC invasion and metastasis *in vitro*

The cell migration and invasion assays demonstrated that c-Src inhibition via PP2 (5 μM) suppressed the migration and invasion capacity of SCC1483 and YD15 cell lines across

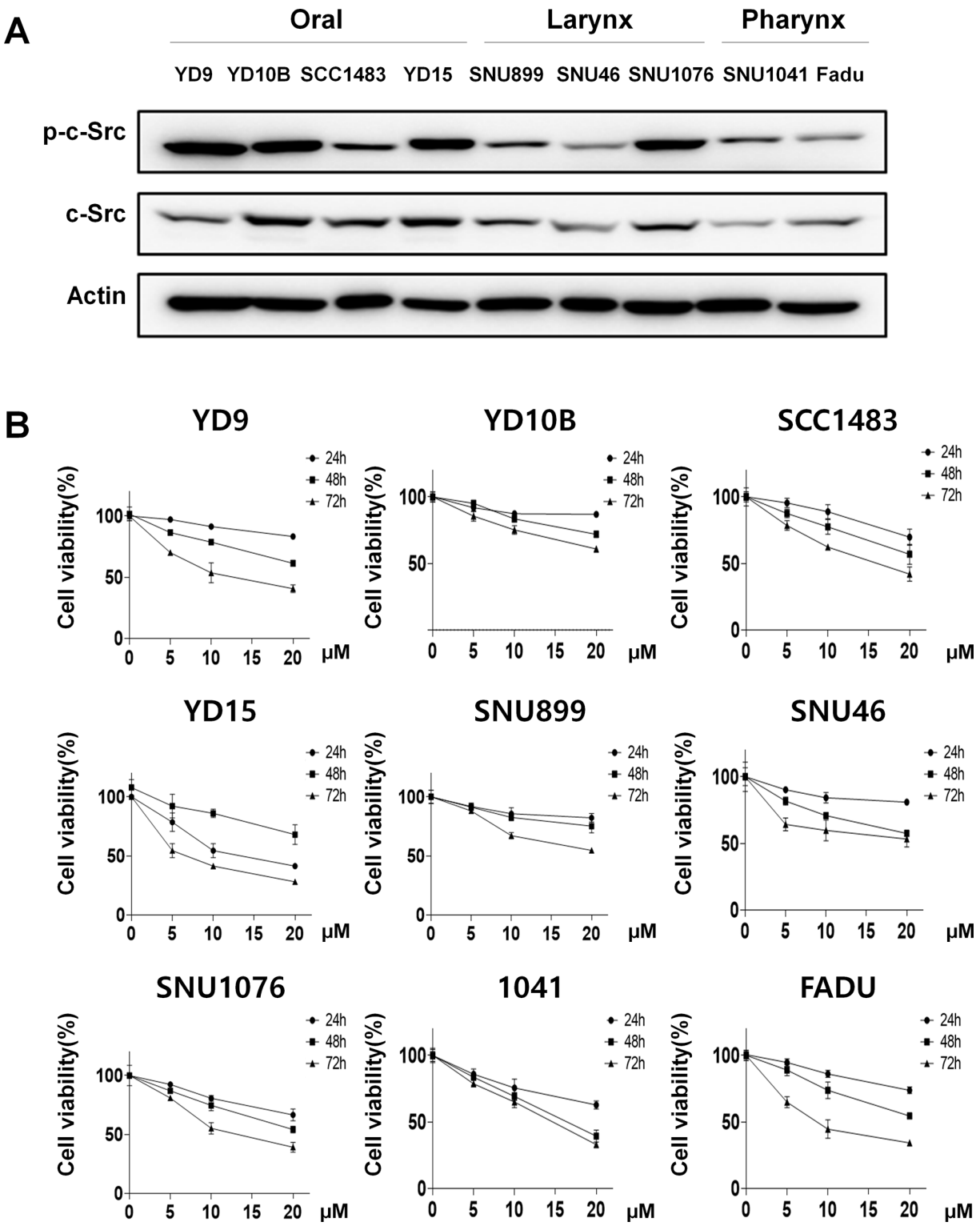

Figure 1. c-Src phosphorylation in head and neck squamous cell carcinoma (HNSCC) cell lines and c-Src inhibition via PP2. (A) Immunoblotting of phosphorylated and total c-Src expression in nine HNSCC cell lines. (B) Cell proliferation assay. SNU1041, FaDu, SNU46, SNU1076, SNU899, SCC1483, YD15, YD9, and YD10-B were incubated with vehicle, 5, 10, or 20 μM PP2 for 24, 48, or 72 h. A cell viability assay was then performed. Different letters indicate a significant difference ($p < 0.05$) based on one-way ANOVA and Turkey's honestly significant difference (HSD) test. Each assay was performed in triplicate, and data are presented as the mean ± standard error of the mean. NS: not significant.

the scratched area relative to the control conditions (Figure 3(a) and (b)). PP2 inhibited tumor cell migration by 15% in SCC1483 and 35.83% in YD15 cells after incubating 24 h (Figure 3(a)). The invasion capacity decreased 2.5-fold in SCC1483 and 2.0-fold in YD15 cells compared with controls (Figure 3(b)). Therefore, it can be inferred that c-Src inhibition

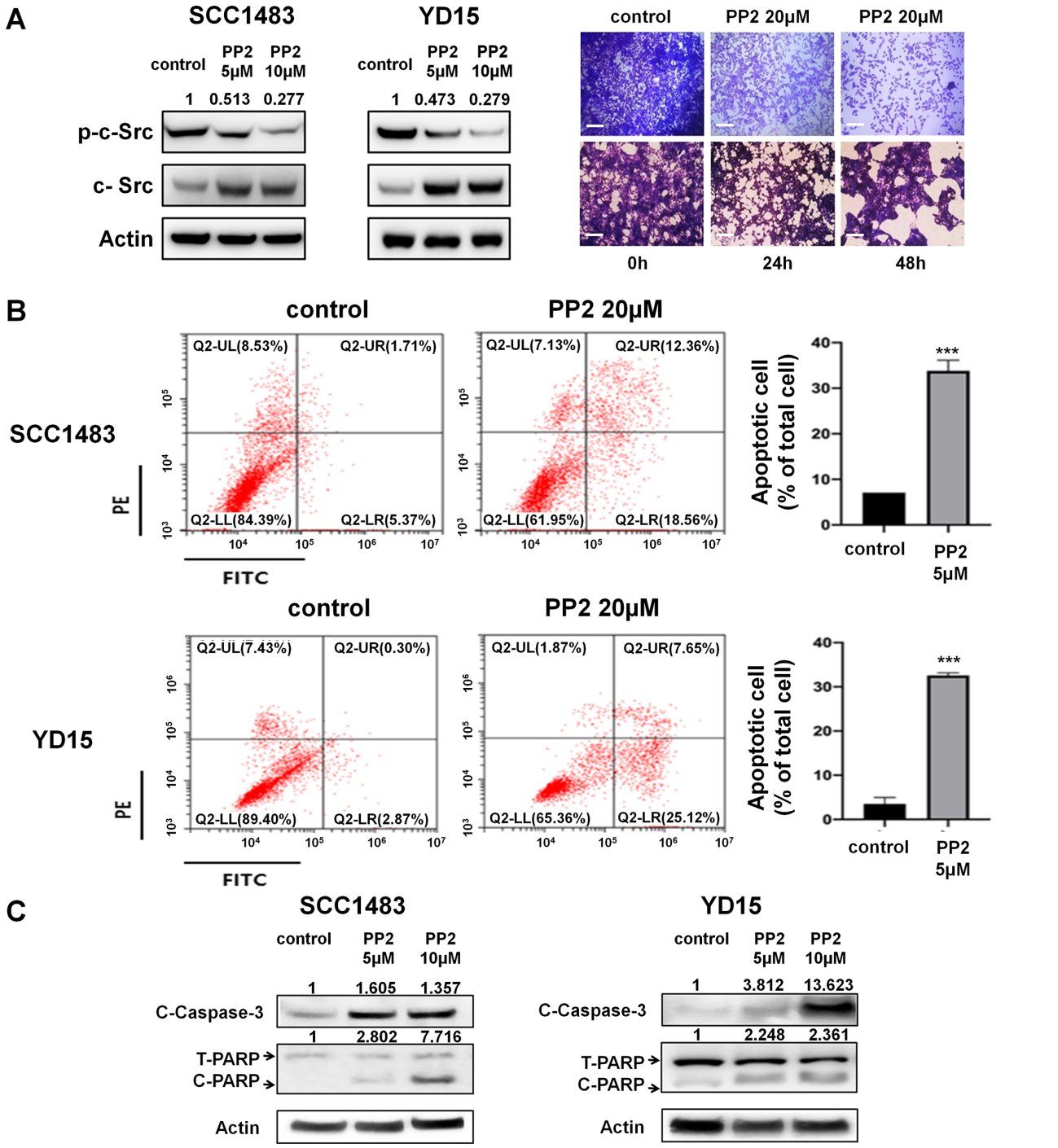

Figure 2. Cell proliferation of SCC1483 and YD15 cells. (A) Immunoblotting of phosphorylated and total c-Src in SCC1483 and YD15 cells treated with 5 or 10 μM PP2 for 24 h. (B) Apoptotic cells in SCC1483 and YD15 cells treated with PP2. The cells were treated with PP2 (10 μM) for 24 h. Afterward, annexin V/PI staining and flow cytometry were performed to assess apoptosis. Values show the percentage of cells in the annexin (early apoptotic; lower right) and annexin/PI (late apoptotic; upper right) quadrants (left panel). The graph shows a significant increase in apoptotic cells among PP2-treated SCC1483 and YD15 cells (right panel). (C) Immunoblotting of cleaved caspase-3 in SCC1483 and YD15 cells treated with 5 or 10 μM PP2 for 24 h. *$p < 0.05$; ** $p < 0.01$; *** $p < 0.001$; Scale bar = 250 μm. β-Actin was used as a loading control in all western blots.

by PP2 effectively suppressed not only tumor cell growth but also HNSCC invasion and metastasis.

PP2 downregulates the epithelial–mesenchymal transition (EMT) in HNSCC

As PP2 suppressed tumor cell invasion and migration, we assessed EMT-associated protein expression in SCC1483 and YD15 cell lines. The results showed that the EMT-related proteins such as N-cadherin, vimentin, Slug, Snail, Erk, and Akt were downregulated, and E-cadherin was significantly upregulated in PP2-treated SCC1483 and YD15 cells compared with controls (Figure 3(c) and (d)). These results suggest that PP2 suppresses HNSCC progression by regulating EMT signaling, including Erk, Akt/Slug, and Snail/E-cadherin.

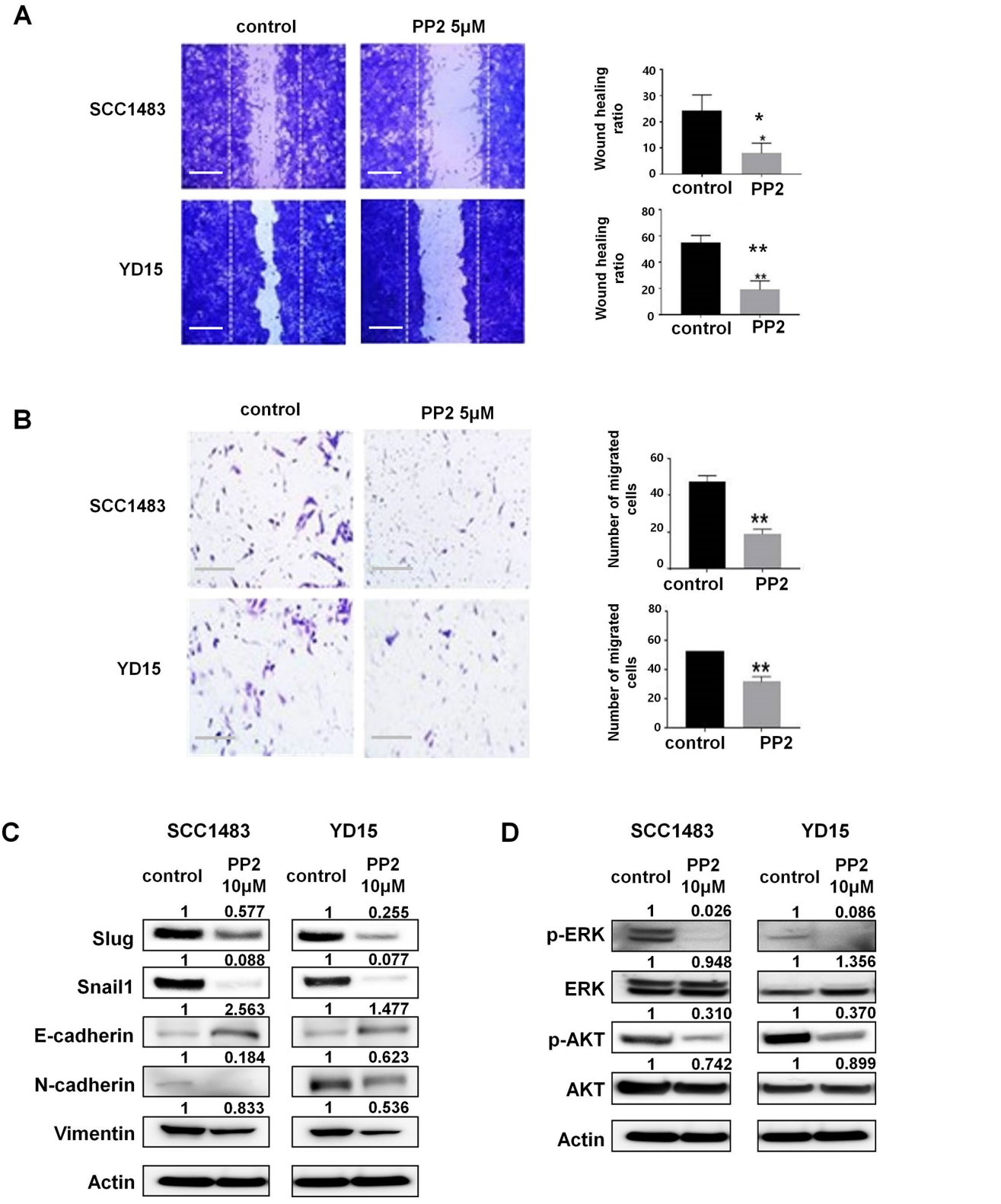

Figure 3. PP2 suppresses cell migration and invasion and downregulated EMT pathway proteins in SCC1483 and YD15 cells. (A) Wound-healing assay. The effects of PP2 on wound healing were evaluated via crystal violet staining after 24 h under ×100 magnification (left panel). Quantitative analyses of wound-healing ratios are shown in the right panel. (B) Invasion assay. Cell lines were seeded on a filter (pore size, 8 μm) coated with Matrigel in the upper chamber of a Transwell plate and exposed to 5 μM PP2. After 24 h, cells attached to the lower section were stained with crystal violet (left panel) and examined at ×200 magnification. (C) Immunoblotting of Slug, Snail, E-cadherin, N-cadherin, and vimentin in SCC1483 and YD15 cells treated with 10 μM PP2 for 24 h. (D) Immunoblotting of pERK, ERK, pAKT, and AKT in SCC1483 and YD15 cells treated with 10 μM PP2 for 24 h. (A, B) Each assay was performed in triplicate independently. Data represent the mean ± standard error of the mean. *$p < 0.05$, ** $p < 0.01$, *** $p < 0.001$; Scale bar = 250 μm. β-Actin was used as a loading control in all western blots.

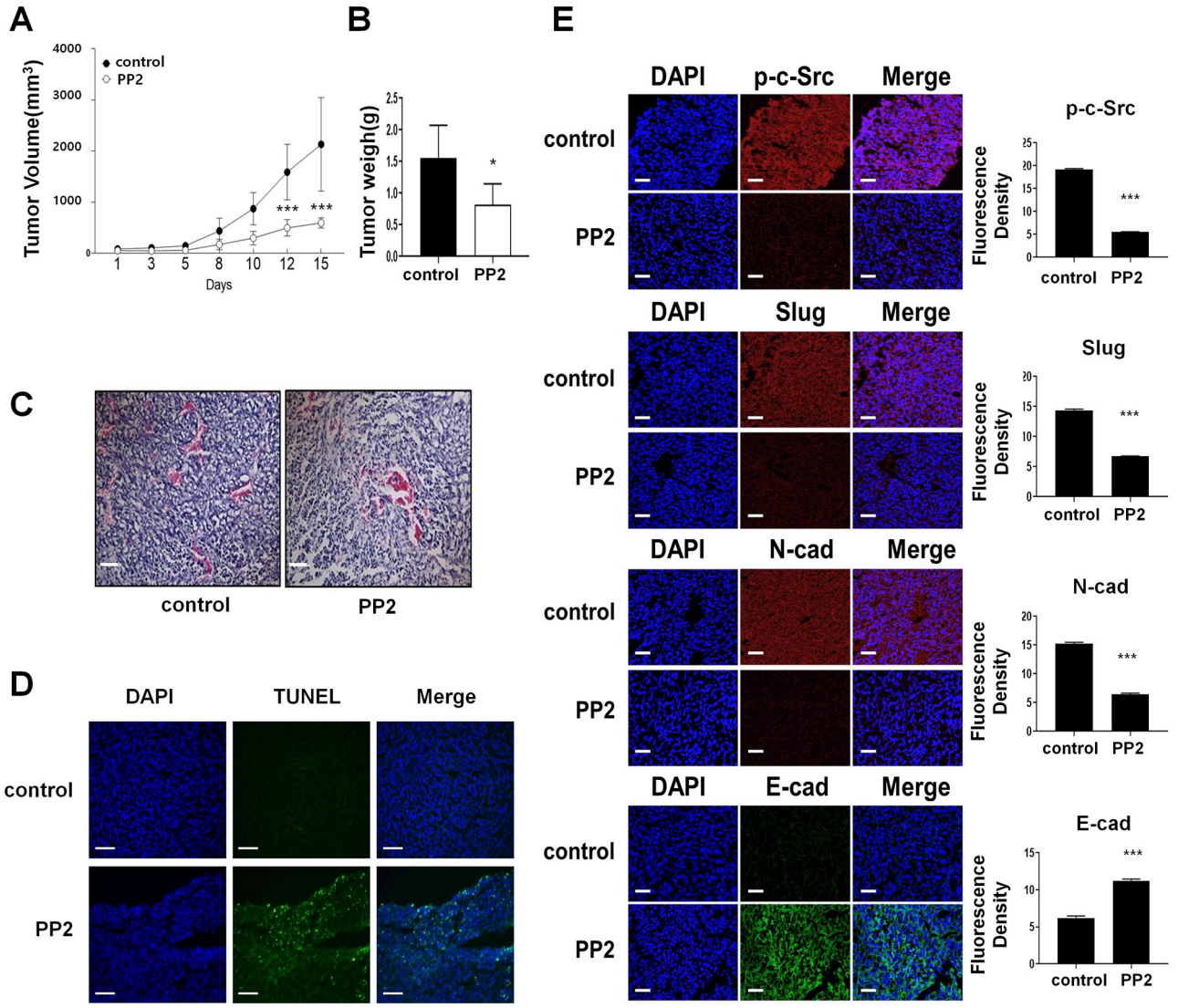

Figure 4. Therapeutic effects of PP2 in the SCC1483 xenograft mouse model. (A) Tumor growth. The tumor volumes were 100–200 mm^3 at the start of treatment. Tumor size was measured after PP2 treatment once every 2 days for 15 days. (B) Tumor weight (C). Hematoxylin-eosin staining of tumor tissues of control and PP2-treated tumor-bearing mouse. (D) Tumor tissue sections from PP2-treated mice were subjected to TUNEL assays for apoptosis detection. (E) Immunofluorescence of p-c-Src (red), slug (red), N-cadherin (red), and E-cadherin (green) in representative tumor tissue sections from PP2-treated mice. *$p < 0.05$, ** $p < 0.01$, *** $p < 0.001$; Scale bar = 250 µm.

Therapeutic effects of PP2 on the SCC1483 xenograft mouse model

To determine whether PP2 treatment would suppress HNSCC *in vivo*, we established the SCC1483 human HNSCC xenograft mouse model. Evaluation of the efficacy of PP2 treatment to suppress HNSCC in vivo in xenograft mice model demonstrated reduced tumor growth in PP2-treated mice than in control mice ($p = 0.0005$; Figure 4). Furthermore, a significant change in tumor size and weight was observed (Figure 4(a) and (b)). Hematoxylin and eosin staining of the excised tumors highlighted tumor heterogeneity between PP2-treated mice (Figure 4(c)). In addition, the number of TUNEL-positive cells was significantly increased in the tumors of PP2-treated mice (Figure 4(d)). These results indicated that PP2-mediated apoptosis plays a significant role in HNSCC. The assessment of the p-c-Src and EMT marker expression levels using immunofluorescence staining revealed significantly reduced levels of p-c-Src and mesenchymal markers, slug and N-cadherin, in a dose-dependent manner, and increased levels of the epithelial marker E-cadherin in the tumors of PP2-treated mice than those in control mice (Figure 4(e)).

Discussion

Management of HNSCC includes single treatment or combination regimens incorporating surgery, chemotherapy, radiation, targeted therapy, and immunotherapy. However, these regimes have respective limitations, necessitating further research to optimize cancer treatment. There has been considerable research into targeted therapy approaches for HNC. This study demonstrated that PP2-mediated inhibition of c-Src impeded tumor cell growth and progression by regulating EMT signaling in HNSCC.

PP2 is a c-Src selective inhibitor whose effect on HNSCC has not been extensively studied due to the poor clinical efficacy of other well-studied tyrosine kinase inhibitors[12,14,15] PP2 is a pan-Src kinase inhibitor, which acts less selectively and is structurally different from selective Src inhibitors such as dasatinib. The lack of selectivity of PP2 has intricated the interpretation of the results of several studies evaluating PP2, as the inhibitory effects could also be attributed to the inhibition of many other kinases.[28,29] Nevertheless, the inhibition of c-Src activity with PP2 demonstrated the therapeutic anticancer effect by restoring cetuximab sensitivity in gastric and colorectal cancers.[17,30] Therefore, we decided to investigate the effects of PP2 on HNSCC.

First, we determined the phosphorylated and total c-Src levels in nine HNSCC cell lines to screen for c-Src-hyperactive HNSCC. c-Src phosphorylation was prominent in SCC1483, YD15, and SNU899 cells.[31] Furthermore, our findings demonstrated that PP2 suppressed the growth, migration, and invasion capacity of SCC1483 and YD15 cell lines. PP2 treatment increased the cleaved caspase-3 and cleaved PARP levels in SCC1483 and YD15 cells.

Several studies have reported the relation between EMT and drug resistance in multiple cancers, including HNSCC.[32–35] Reportedly, in cells undergoing EMT, epithelial factors, such as tight junction protein 1 and E-cadherin, are downregulated. In contrast, the mesenchymal factors, such as vimentin and N-cadherin, are upregulated.[36] In this study, we analyzed the factors related to the EMT pathway to clarify the mechanism of the observed effects of PP2. Of the EMT markers, slug, a transcription factor that induces EMT, has been shown to related caspase-9 activity in cancer cells.[37] Restoring E-cadherin expression in lung cancer cell lines increased the sensitivity to EGFR inhibitors.[38] Maseki *et al.* reported the acquisition of the EMT phenotype in EGFR-resistant HNSCC cell lines through Akt/Snail signaling.[39]

c-Src has also been linked to EMT in lung carcinomas, wherein c-Src is overexpressed or hyper-activated.[40] c-Src has been demonstrated to play a key role in the regulation of EMT via acting through the Erk, Akt/Slug, and Snail/E-cadherin cascades.[41,42] Therefore, PP2 was expected to inhibit EMT-related factors downstream of c-Src, suppressing the transition. Here, we showed that Erk and Akt were downregulated in PP2-treated cells, as were Slug and Snail, whereas the expression of E-cadherin was upregulated. These results suggest PP2 regulates EMT signaling, downregulating invasive and metastatic potential of HNSCC cell lines.

In conclusion, this study indicates that PP2 is a potential therapeutic candidate for HNSCC, which acts via regulation of the EMT signaling pathway and c-Src. These findings highlight the efficiency of c-Src as a potential therapeutic target for treating HNSCC.

AUTHORS' CONTRIBUTIONS

SYL and SJP contributed equally to this work. The study was designed by YSK, SJP, and BSL. SJP and SYL performed the experiments. The data were analyzed by SJP, SYL, JSR, JGK, BSL, and CHK. SJP, SYL, SMS, and IHK prepared the manuscript. All authors read and approved the final manuscript.

DECLARATION OF CONFLICTING INTERESTS

The author(s) declared no potential conflicts of interest with respect to the research, authorship, and/or publication of this article.

FUNDING

The author(s) disclosed receipt of the following financial support for the research, authorship, and/or publication of this article: This work was supported by a grant from Konyang University Myunggok Medical Research Institute (Myunggok 18-02) and National Research Foundation of Korea (NRF) grant funded by the Korea government (MSIT) (NRF-2019R1F1A1059118).

ORCID ID

Yeon Soo Kim https://orcid.org/0000-0002-7862-1662

REFERENCES

1. Jou A, Hess J. Epidemiology and molecular biology of head and neck cancer. *Oncol Res Treat* 2017;**40**:328–32
2. Mery B, Rancoule C, Guy JB, Espenel S, Wozny AS, Battiston-Montagne P, Ardail D, Beuve M, Alphonse G, Rodriguez-Lafrasse C, Magne N. Preclinical models in HNSCC: a comprehensive review. *Oral Oncol* 2017;**65**:51–6
3. Thomas SM, Brugge JS. Cellular functions regulated by Src family kinases. *Annu Rev Cell Dev Biol* 1997;**13**:513–609
4. Brown MT, Cooper JA. Regulation, substrates and functions of src. *Biochim Biophys Acta* 1996;**1287**:121–49
5. Irby RB, Yeatman TJ. Role of Src expression and activation in human cancer. *Oncogene* 2000;**19**:5636–42
6. Zhang Q, Thomas SM, Xi S, Smithgall TE, Siegfried JM, Kamens J, Gooding WE, Grandis JR. SRC family kinases mediate epidermal growth factor receptor ligand cleavage, proliferation, and invasion of head and neck cancer cells. *Cancer Res* 2004;**64**:6166–73
7. Ke L, Xiang Y, Guo X, Lu J, Xia W, Yu Y, Peng Y, Wang L, Wang G, Ye Y, Yang J, Liang H, Kang T, Lv X. c-Src activation promotes nasopharyngeal carcinoma metastasis by inducing the epithelial-mesenchymal transition via PI3K/Akt signaling pathway: a new and promising target for NPC. *Oncotarget* 2016;**7**:28340–55
8. Ishizawar R, Parsons SJ. c-Src and cooperating partners in human cancer. *Cancer Cell* 2004;**6**(3):209–14
9. Mandal M, Myers JN, Lippman SM, Johnson FM, Williams MD, Rayala S, Ohshiro K, Rosenthal DI, Weber RS, Gallick GE, El-Naggar AK. Epithelial to mesenchymal transition in head and neck squamous carcinoma: association of Src activation with E-cadherin down-regulation, vimentin expression, and aggressive tumor features. *Cancer* 2008;**112**:2088–100
10. Koppikar P, Choi SH, Egloff AM, Cai Q, Suzuki S, Freilino M, Nozawa H, Thomas SM, Gooding WE, Siegfried JM, Grandis JR. Combined inhibition of c-Src and epidermal growth factor receptor abrogates growth and invasion of head and neck squamous cell carcinoma. *Clin Cancer Res* 2008;**14**:4284–91
11. Puls LN, Eadens M, Messersmith W. Current status of SRC inhibitors in solid tumor malignancies. *Oncologist* 2011;**16**(5):566–78
12. Fury MG, Baxi S, Shen R, Kelly KW, Lipson BL, Carlson D, Stambuk H, Haque S, Pfister DG. Phase II study of saracatinib (AZD0530) for patients with recurrent or metastatic head and neck squamous cell carcinoma (HNSCC). *Anticancer Res* 2011;**31**:249–53
13. Johnson FM, Saigal B, Talpaz M, Donato NJ. Dasatinib (BMS-354825) tyrosine kinase inhibitor suppresses invasion and induces cell cycle arrest and apoptosis of head and neck squamous cell carcinoma and non-small cell lung cancer cells. *Clin Cancer Res* 2005;**11**:6924–32
14. Brooks HD, Glisson BS, Bekele BN, Johnson FM, Ginsberg LE, El-Naggar A, Culotta KS, Takebe N, Wright J, Tran HT, Papadimitrakopoulou VA. Phase 2 study of dasatinib in the treatment of head and neck squamous cell carcinoma. *Cancer* 2011;**117**:2112–9

15. Wheeler DL, Iida M, Kruser TJ, Nechrebecki MM, Dunn EF, Armstrong EA, Huang S, Harari PM. Epidermal growth factor receptor cooperates with Src family kinases in acquired resistance to cetuximab. *Cancer Biol Ther* 2009;**8**(8):696–703
16. Song N, Liu S, Zhang J, Liu J, Xu L, Liu Y, Qu X. Cetuximab-induced MET activation acts as a novel resistance mechanism in colon cancer cells. *Int J Mol Sci* 2014;**15**:5838–51
17. Li X, Xu L, Li H, Zhao L, Luo Y, Zhu Z, Liu Y, Qu X. Cetuximab-induced insulin-like growth factor receptor I activation mediates cetuximab resistance in gastric cancer cells. *Mol Med Rep* 2015;**11**(6):4547–54
18. Stabile LP, He G, Lui VW, Thomas S, Henry C, Gubish CT, Joyce S, Quesnelle KM, Siegfried JM, Grandis JR. c-Src activation mediates erlotinib resistance in head and neck cancer by stimulating c-Met. *Clin Cancer Res* 2013;**19**:380–92
19. Lieu C, Kopetz S. The SRC family of protein tyrosine kinases: a new and promising target for colorectal cancer therapy. *Clin Colorectal Cancer* 2010;**9**(2):89–94
20. Zhang L, Teng Y, Zhang Y, Liu J, Xu L, Qu J, Hou K, Yang X, Liu Y, Qu X. C-Src-mediated RANKL-induced breast cancer cell migration by activation of the ERK and Akt pathway. *Oncol Lett* 2012;**3**(2):395–400
21. Eom KY, Cho BJ, Choi EJ, Kim JH, Chie EK, Wu HG, Kim IH, Paek SH, Kim JS, Kim IA. The effect of chemoradiotherapy with SRC tyrosine kinase inhibitor, PP2 and temozolomide on malignant glioma cells in vitro and in vivo. *Cancer Res Treat* 2016;**48**(2):687–97
22. Kong L, Deng Z, Shen H, Zhang Y. Src family kinase inhibitor PP2 efficiently inhibits cervical cancer cell proliferation through down-regulating phospho-Src-Y416 and phospho-EGFR-Y1173. *Mol Cell Biochem* 2011;**348**(1–2):11–9
23. Lee BS, Kang S, Kim KA, Song YJ, Cheong KH, Cha HY, Kim CH. Met degradation by SAIT301, a Met monoclonal antibody, reduces the invasion and migration of nasopharyngeal cancer cells via inhibition of EGR-1 expression. *Cell Death Dis* 2014;**5**:e1159
24. Kang SU, Seo SJ, Kim YS, Shin YS, Koh YW, Lee CM, Yang SS, Lee JS, Moon E, Kang H, Ryeo JB, Lee Y, Kim CH. Comparative effects of non-thermal atmospheric pressure plasma on migration and invasion in oral squamous cell cancer, by gas type. *Yonsei Med J* 2017;**58**(2):272–81
25. Lim YC, Park HY, Hwang HS, Kang SU, Pyun JH, Lee MH, Choi EC, Kim CH. (-)-Epigallocatechin-3-gallate (EGCG) inhibits HGF-induced invasion and metastasis in hypopharyngeal carcinoma cells. *Cancer Lett* 2008;**271**:140–52
26. Ma YC, Shi C, Zhang YN, Wang LG, Liu H, Jia HT, Zhang YX, Sarkar FH, Wang ZS. The tyrosine kinase c-Src directly mediates growth factor-induced Notch-1 and Furin interaction and Notch-1 activation in pancreatic cancer cells. *PLoS ONE* 2012;**7**(3):e33414
27. Kim M, Jung K, Kim IS, Lee IS, Ko Y, Shin JE, Park KI. TNF-alpha induces human neural progenitor cell survival after oxygen-glucose deprivation by activating the NF-kappaB pathway. *Exp Mol Med* 2018;**50**:1–14
28. Williams NK, Lucet IS, Klinken SP, Ingley E, Rossjohn J. Crystal structures of the Lyn protein tyrosine kinase domain in its Apo- and inhibitor-bound state. *J Biol Chem* 2009;**284**:284–91
29. Brandvold KR, Steffey ME, Fox CC, Soellner MB. Development of a highly selective c-Src kinase inhibitor. *ACS Chem Biol* 2012;**7**:1393–8
30. Lu Y, Li X, Liang K, Luwor R, Siddik ZH, Mills GB, Mendelsohn J, Fan Z. Epidermal growth factor receptor (EGFR) ubiquitination as a mechanism of acquired resistance escaping treatment by the anti-EGFR monoclonal antibody cetuximab. *Cancer Res* 2007;**67**:8240–7
31. Chang JW, Kang SU, Shin YS, Seo SJ, Kim YS, Yang SS, Lee JS, Moon E, Lee K, Kim CH. Combination of NTP with cetuximab inhibited invasion/migration of cetuximab-resistant OSCC cells: involvement of NF-kappaB signaling. *Sci Rep* 2015;**5**:18208
32. Chang TH, Tsai MF, Su KY, Wu SG, Huang CP, Yu SL, Yu YL, Lan CC, Yang CH, Lin SB, Wu CP, Shih JY, Yang PC. Slug confers resistance to the epidermal growth factor receptor tyrosine kinase inhibitor. *Am J Respir Crit Care Med* 2011;**183**:1071–9
33. Shang Y, Cai X, Fan D. Roles of epithelial-mesenchymal transition in cancer drug resistance. *Curr Cancer Drug Targets* 2013;**13**:915–29
34. Singh A, Settleman J. EMT, cancer stem cells and drug resistance: an emerging axis of evil in the war on cancer. *Oncogene* 2010;**29**:4741–51
35. Sequist LV, Waltman BA, Dias-Santagata D, Digumarthy S, Turke AB, Fidias P, Bergethon K, Shaw AT, Gettinger S, Cosper AK, Akhavanfard S, Heist RS, Temel J, Christensen JG, Wain JC, Lynch TJ, Vernovsky K, Mark EJ, Lanuti M, Iafrate AJ, Mino-Kenudson M, Engelman JA. Genotypic and histological evolution of lung cancers acquiring resistance to EGFR inhibitors. *Sci Transl Med* 2011;**3**:75ra26
36. Lamouille S, Xu J, Derynck R. Molecular mechanisms of epithelial-mesenchymal transition. *Nat Rev Mol Cell Biol* 2014;**15**:178–96
37. Jiang F, Zhou L, Wei C, Zhao W, Yu D. Slug inhibition increases radiosensitivity of oral squamous cell carcinoma cells by upregulating PUMA. *Int J Oncol* 2016;**49**(2):709–19
38. Witta SE, Gemmill RM, Hirsch FR, Coldren CD, Hedman K, Ravdel L, Helfrich B, Dziadziuszko R, Chan DC, Sugita M, Chan Z, Baron A, Franklin W, Drabkin HA, Girard L, Gazdar AF, Minna JD, Bunn PA Jr. Restoring E-cadherin expression increases sensitivity to epidermal growth factor receptor inhibitors in lung cancer cell lines. *Cancer Res* 2006;**66**:944–50
39. Maseki S, Ijichi K, Tanaka H, Fujii M, Hasegawa Y, Ogawa T, Murakami S, Kondo E, Nakanishi H. Acquisition of EMT phenotype in the gefitinib-resistant cells of a head and neck squamous cell carcinoma cell line through Akt/GSK-3beta/snail signalling pathway. *Br J Cancer* 2012;**106**:1196–204
40. Guarino M. Src signaling in cancer invasion. *J Cell Physiol* 2010;**223**:14–26
41. Patel A, Sabbineni H, Clarke A, Somanath PR. Novel roles of Src in cancer cell epithelial-to-mesenchymal transition, vascular permeability, microinvasion and metastasis. *Life Sci* 2016;**157**:52–61
42. Liu X, Feng R. Inhibition of epithelial to mesenchymal transition in metastatic breast carcinoma cells by c-Src suppression. *Acta Biochim Biophys Sin* 2010;**42**(7):496–501

(Received May 1, 2022, Accepted October 5, 2022)